Protection Level Formulations for Distance Measuring Equipment (DME)

Brandon Weaver, Gianluca Zampieri, Okuary Osechas, *German Aerospace Center (DLR)*

BIOGRAPHY

Brandon Weaver is a researcher at the German Aerospace Center (DLR) where he investigates topics concerning alternative position, navigation, and time (APNT) to complement and backup GNSS systems. He received his master's degree in Mechanical Engineering from Tufts University in 2020 as a Draper Fellow. Prior to attending Tufts, he worked at Draper supporting the test and evaluation of GPS receivers. He graduated in 2016 from Auburn University with a bachelor's degree in Mechanical Engineering.

Gianluca Zampieri received a Master degree in Electronics and Telecommunications Engineering from University of Trento, Italy in 2019. After graduation, he joined the Alternative Navigation Systems Group at the Institute for Communication and Navigation of the German Aerospace Centre (DLR). He is involved in the SESAR activities related to APNT, first as project manager and recently as technical advisor. In addition, he is currently pursuing his Ph.D. degree at the RWTH Aachen University.

Okuary Osechas is a researcher with the Institute of Communications and Navigation at DLR and leads the Alternative Navigation Systems group. He received a Diploma in Electrical Engineering from Karlsruhe University and a Ph.D. in Electrical Engineering from Tufts University.

ABSTRACT

This paper derives protection level (PL) formulations of Distance Measuring Equipment (DME) starting from a general framework to assure their applicability to DME systems. DME is seen as a potential Required Navigation Performance (RNP) system to be used in the scenario that GPS and other Global Navigation Satellite Systems (GNSS) are unavailable. Since prior evaluations used PL formulations originally developed for augmented GNSS, we investigate the validity of certain assumptions made for GNSS as applied to DME by deconstructing the formulations according to the general PL framework. DME, for example, contains station monitoring that automatically shuts down stations transmitting out-of-tolerance signals which is not the case for standalone GPS. We provide an argument justifying a DME PL for the fault-free and single-fault conditions only, and present an integrity evaluation for DME using these PLs and the current DME network in Europe. The results suggest that DME is a viable RNP alternative when able to compute the PLs in real-time.

1. INTRODUCTION

When GPS was first being evaluated for navigation capability in civil aviation, one of the preeminent concerns was the lack of timely monitoring of the transmitted signals. While the existing navigation infrastructure, e.g. Distance Measuring Equipment (DME), included executive monitors that could shut off stations detected to transmit out-of-tolerance signals within seconds, standalone GPS had no such capability. This concern motivated the conception and development of *integrity* as a system parameter by which to evaluate navigation system performance.

As augmentations to GPS were developed to improve its integrity performance, the integrity concept itself evolved to coincide with the transition of navigation requirements to be specified in terms of aircraft-level performance rather than mandatory equipage. An integrity performance metric known as *protection level* (PL) was conceived to allow direct comparison with an *alert limit* (AL), specified as part of integrity requirements, to evaluate compliance with those requirements. A PL is generally described as a confidence bound on the assured position error, and the formulations proposed were developed specifically for the various GPS augmentations.

Nowadays, multiple Global Navigation Satellite Systems (GNSS) exist with their own corresponding augmentations that can be used for navigation. However, there is an increasing awareness that an alternative or complement system to GNSS is a

 https://doi.org/10.33012/2023.18587

prudent option to have due to GNSS outage incidents affecting civil aviation. One obvious solution is continued usage of legacy navigation systems, particularly DME, to provide a similar level of navigation performance in the case that GNSS is unavailable. This targeted level of performance is referred to as Required Navigation Performance (RNP), and includes the mandatory capability of on-board performance monitoring and alerting (OPMA).

Evaluations of DME have been undertaken to demonstrate its feasibility as a potential RNP system. Since integrity is one of the more stringent requirements, PLs are commonly used in these evaluations to characterize DME integrity performance as an overall measure of RNP capability. In addition to predicting a level of integrity performance, such formulations are used to enable OPMA for integrity if computed in real-time by the on-board system. The PL formulations are typically adopted from augmented GNSS without much discussion as to their applicability to DME, implicitly making assumptions that might be valid for GNSS but have not been fully justified for non-GNSS systems.

This paper identifies these implicit assumptions by applying a general protection level framework to DME in the process of formulating a PL. First, a model of integrity is described so that integrity requirements can be understood. Next, the standard framework for general protection levels is presented before being applied to DME in particular. The fault conditions warranting a protection level are determined, with the appropriate PLs being discussed in more detail. Finally, the results of an evaluation of integrity using PLs is presented for the DME network in Europe.

2. INTEGRITY MODEL

This section describes an interpretation of integrity requirements presented in Joerger et al. (2014) as well as Pullen and Joerger (2021). A loss of integrity, LOI, occurs when a position error exceeding some alert limit (AL) goes unannounced. Let A be the event that a timely alert is raised and PF_{AL} the event of a position failure, i.e. a position error exceeding a region defined by the AL. The loss of integrity event is then defined as the intersection of the events PF_{AL} and A' (no timely alert):

$$LOI = A' \cap PF_{AL} \tag{1}$$

Now consider a set of mutually exclusive fault conditions, $\{H_i\}$, that partition the certain event (i.e. the event containing all possible outcomes), Ω, so that

$$\bigcup_i H_i = \Omega \tag{2}$$

is true. For example, the collection $\{H_0, H_1\}$ with H_0 being the fault-free condition and H_1 being the at-least-one-fault condition would result in $\bigcup_{i=0}^{1} H_i = \Omega$. By the law of total probability, the probability of LOI, $P(LOI)$, can be expressed as a sum of joint probabilities with each fault condition H_i:

$$P(LOI) = \sum_i P(LOI \cap H_i) = \sum_i P(A' \cap PF_{AL} \cap H_i) \tag{3}$$

Joint probabilities can be expressed as the product of conditional probabilities, so that (3) becomes:

$$P(LOI) = \sum_i P(H_i) P(LOI|H_i) = \sum_i P(H_i)\, P(A' \cap PF_{AL}|H_i) \tag{4}$$

Navigation requirements specify a maximum allowable $P(LOI)$ for a given AL and time-to-alert (TTA), which is the time interval after the occurrence of a position failure in which an alert is considered timely. This maximum allowable probability, called the integrity risk (I_{risk}), contributes to the integrity requirement along with the specified AL and TTA. Expressed symbolically, the integrity requirement I_{REQ} is

$$I_{REQ} = (I_{risk}, AL, TTA) \tag{5}$$

where the condition

$$P(LOI) < I_{risk} \tag{6}$$

must be met for a navigation system to be considered compliant with the integrity requirement.

3. PROTECTION LEVEL CONCEPT

Integrity can be evaluated by computing $P(LOI)$ for a specified AL and TTA and directly checking that condition (6) holds. Alternatively, integrity can be evaluated by deriving a protection level that defines the region containing the position error with the required integrity. This protection level (PL) is then compared to the specified AL; should the AL encompass the PL region, then the integrity requirement is said to be met. This allows a more convenient integrity evaluation method for multiple AL specifications simultaneously, and can be used (i) to predict coverage/availability of a system (ii) onboard an aircraft for real-time monitoring of performance (Pullen & Joerger, 2021).

Therefore, the condition for compliancy with the integrity requirement can be reformulated from (6) such that the condition to be met is

$$PL < AL \tag{7}$$

where PL defines the region such that

$$P(LOI) = \sum_i P(H_i)P(A' \cap PF_{PL}|H_i) < I_{risk} \tag{8}$$

with PF_{PL} defined as the event that the position error exceeds the PL region.

A PL generally applies to a particular fault condition. For each H_i, a PL_i is then derived such that

$$P(LOI \cap H_i) = P(H_i)P\left(A' \cap PF_{PL_i}|H_i\right) < I_{risk,i} \tag{9}$$

where $I_{risk,i}$ is a portion of I_{risk} allocated to $P(LOI \cap H_i)$. Allocation of I_{risk} ensures that the largest PL_i can be taken as the effective PL, since $\max[PL_i]$ bounds the position error with its allocated $I_{risk,i}$ as well as the allocation of any smaller PL_i. Since the sum of the allocations equal I_{risk}, $\max[PL_i]$ also satisfies I_{risk}.

3.1. Determining relevant fault conditions

The first step in formulating PLs is determining how to partition the LOI event into fault conditions. A fault in this paper is simply an out-of-tolerance measurement, e.g. DME slant-range. An initial partition consists of the fault-free condition (H_0), the single-fault condition (H_1), and the multiple simultaneous fault condition (H_2). The joint probability of LOI due to each fault condition, $P(LOI \cap H_i)$, should be compared to the specified I_{risk} to determine which fault conditions actually warrant a PL. In other words, for those conditions where $P(LOI \cap H_i) \ll I_{risk}$, their occurrence is deemed so unlikely as to not need a protection level.

One approach to determine the relevant fault conditions is described in Appendix A of Joerger et al. (2014). First, since $P\left(A' \cap PF_{PL_i}|H_i\right) \leq 1$, by (9) the joint probability $P(LOI \cap H_i)$ can be upper bounded with $P(H_i)$ alone, simplifying the computation. Next, $P(H_i)$ is simply the probability of zero, exactly one, or multiple measurement faults for H_0, H_1, and H_2 respectively. If each measurement has an equal fault probability of p, the number of k simultaneous measurement faults in n measurements can be modeled as having a Binomial distribution:

$$P(k) = \binom{n}{k}(1-p)^{n-k}p^k \tag{10}$$

The above formula relates back to the fault conditions with $P(H_0) = P(k = 0)$, $P(H_1) = P(k = 1)$, and $P(H_2) = P(k \geq 2)$.

If a single-fault is not equally likely for each measurement, such that the jth measurement has a fault probability of p_j, then k has a Poisson-Binomial distribution and quickly becomes impractical to compute as n increases. An upper bound is given in Appendix C of Blanch et al. (2012) for the probability of k or more faults occurring simultaneously for n measurements:

$$P(\geq k) \leq \frac{\left(\sum_{j=1}^{n} p_j\right)^k}{k!} \tag{11}$$

In the case of DME, where each station is independent and there is little justification for not considering equally likely measurement faults, (10) is sufficient for determining appropriate protection levels. In multisensor or hybrid approaches where measurement faults are not equally likely, (11) is the better option.

Before we are able to use the above procedure, we must first determine the specified I_{risk} and the probability of a measurement fault p. The next section begins the process of formulating a DME protection level by first selecting these values.

4. DME PROTECTION LEVELS

Before turning the PL discussion towards DME, a brief description of the system is warranted. DME operates by an airborne interrogator sending out a transmission to a ground station, which responds after a known delay. The elapsed time from sending the interrogation to receiving the reply constitutes a time-of-flight which can be considered a range measurement after including known signal propagation properties. An airborne interrogator capable of scanning multiple DME station frequencies can produce a batch of range measurements that are sufficient for estimating a position, similarly to GNSS. Each DME ground station is paired with at least one executive monitor that can detect the signal performance and, if necessary, shutdown an out-of-tolerance station within seconds (Department of Defense, Department of Transportation, and Department of Homeland Security, 2021).

Our application of PLs to DME apply to the en-route through nonprecision approach modes of flight, such that any reference to PL actually means a horizontal PL (HPL) unless stated otherwise. To determine the fault conditions that warrant a PL, we use (10) to compute the simultaneous fault probabilities and compare with I_{risk}. For RNP systems, the I_{risk} specified for individual aircraft is 10^{-5}/hr (European Organisation for Civil Aviation Equipment [EUROCAE], 2014). For GNSS, the requirement is more stringent at 10^{-7}/hr as a signal-in-space (SIS) fault is likely to affect multiple aircraft simultaneously (International Civil Aviation Organization [ICAO], 2018). A DME station will also serve multiple aircraft, such that an I_{risk} of 10^{-6}/hr for a DME-derived navigation solution is appropriate (Berz & Saini, 2022). Until a definitive value is chosen, however, we select an I_{risk} of 10^{-7}/hr to be conservative.

That leaves a reasonable value for p, the probability of a measurement fault, to be determined. A fault can be caused by a station fault resulting in an out-of-tolerance signal as well as propagation effects such as multipath. Regarding the station failure, a concurrent failure of the monitoring capability must also occur for a DME signal to be faulted upon transmission. This concurrent failure probability can be quantified as a cumulative risk that grows until an End-to-End (ETE) check is performed. Such checks reset the probability of a latent concurrent fault to zero, as in ILS and MLS systems (European and North Atlantic Office of ICAO, 2019). Working Group (WG) 107 of EUROCAE recently determined that a wide variety of DME station monitoring architectures can achieve less than 10^{-6}/hr between ETE checks (Berz & Saini, 2022). Some of the more reliable ground stations even achieve a concurrent failure probability down to 10^{-9}/hr (Berz et al., 2013).

Propagation effects such as multipath also affect the probability of a measurement fault. As the probability of these effects is particularly hard to quantify, certain justifications are made to its exclusion. First, the measurement performance should be specified using some manner of error overbounding, as is done in the case of GNSS pseudoranges (DeCleene, 2000). This effectively increases the threshold of performance, making out-of-tolerance harder to attain. Second, an assumption is made that any propagation effects are even less likely to result in a position failure for the considered modes of flight: en-route through nonprecision approach. A similar assumption was made in deriving GPS integrity requirements (Lee, et al., 1996) These factors result in the assumption that propagation effects have a negligible impact on the probability of a measurement fault.

To determine the relevant fault conditions by computing each $P(H_i)$ in our initial H_0, H_1, H_2 parition and comparing it to I_{risk}, we select the following values based on the preceding discussion: $I_{risk} = 10^{-7}$/hr and $p = 10^{-6}$/hr. Additionally, we include the 10^{-9}/hr as well for p to show the benefits of a wide network of extremely reliable DME monitoring architectures. The final step is to determine the number of measurements, n, in total. This depends on both the airborne DME architecture and current location; therefore, we perform these computations for a range of values. Since more measurements increases the probability of simultaneous failures, we use $n = 20$ as an arbitrary maximum number of measurements that very few airborne DME units are likely to have. The results of this this analysis are shown in Table 1 below.

Table 1

Probability of k simultaneous faults in n measurements

k	$P(k)$, for $p = 1.00\text{x}10^{-6}$/hr			$P(k)$, for $p = 1.00\text{x}10^{-9}$/hr		
	n = 4	n = 8	n = 20	n = 4	n = 8	n = 20
0	~1	~1	~1	~1	~1	~1
1	$4.00\text{x}10^{-6}$	$8.00\text{x}10^{-6}$	$2.00\text{x}10^{-5}$	$4.00\text{x}10^{-9}$	$8.00\text{x}10^{-9}$	$2.00\text{x}10^{-8}$
2	$6.00\text{x}10^{-12}$	$2.80\text{x}10^{-11}$	$1.90\text{x}10^{-10}$	$6.00\text{x}10^{-18}$	$2.80\text{x}10^{-17}$	$1.90\text{x}10^{-16}$
3	$4.00\text{x}10^{-18}$	$5.60\text{x}10^{-17}$	$1.14\text{x}10^{-15}$	$4.00\text{x}10^{-27}$	$5.60\text{x}10^{-26}$	$1.14\text{x}10^{-24}$

The results in Table 1 reveal the fact that $P(k \geq 2) \ll I_{risk}$ regardless of the values of n and p chosen. This in turn means that a multiple fault PL is unwarranted for DME. Expanding (8) to include only the fault-free and single fault conditions results in the integrity condition to be met:

$$P(LOI) = P(LOI \cap H_0) + P(LOI \cap H_1) < I_{risk} \tag{12}$$

Note that if the improved DME monitoring architecture was prevalent, such that $p = 1.00\text{x}10^{-9}$/hr, only the fault-free condition need be covered with a protection level. The mere possibility of propagation effects likely precludes such an approach, but routes and areas subject to regular flight inspections that characterize the airspace might qualify.

Previous aircraft-level integrity evaluations of DME did not perform this process explicitly, but rather directly formulated a fault-free or single-fault PL originally derived for GPS. Justifying that a PL for H_2 is unwarranted is our first step in connecting the general PL framework to the DME system. The next sections discuss the fault-free and single-fault PL formulations in more detail.

4.1. Fault-Free Protection Level

As the name implies, this type of PL is used to bound the position error with the required integrity in the case that no faulted measurement is present. Such a PL was used to evaluate DME as part of a hybrid system in Lo, et al. (2014). This is also the type of PL used in GNSS systems enabled with Space-Based Augmentation Systems (SBAS), which includes ground monitoring of faults and transmits corrections to aircraft so that a faulted measurement caused by a satellite failure is unlikely (Walter et al., 1999). Propagation effects are mitigated by determining the Gaussian overbounding variance for such errors, thereby increasing the threshold for a measurement to be out-of-tolerance, i.e. faulted (DeCleene, 2000). The condition that $P(LOI \cap H_0)$ is less than the allocated integrity risk must be true for the PL to be valid. The next paragraphs show how the PL region is related to this constraint.

To connect the PL to $P(LOI \cap H_0)$, this term is first expanded using (9) to make the fault-free PL assumptions explicit:

$$P(LOI \cap H_0) = P(H_0)P(A' \cap PF_{PL}|H_0) \tag{13}$$

Since the fault-free condition has no faults to detect onboard the aircraft, it is typical to assume that $P(A'|H_0) = 1$. Additionally, the fault-free condition is almost always the case, such that $P(H_0) = 1$. These assumptions allow us to bound (13) so that

$$P(LOI \cap H_0) \leq P(PF_{PL}|H_0) < I_{risk,0} \tag{14}$$

where $I_{risk,0}$ is the portion of I_{risk} allocated to the fault-free PL. The fault-free PL must then define the region such that the probability of a position failure exceeding this region is less than the allocated integrity risk. By overbounding the measurement errors with a Gaussian distribution, the position error in the horizontal domain has a bivariate Gaussian distribution. This allows one to compute a position error ellipse for a given station geometry using covariance propagation to bound a certain probability of the position error (Mertikas, 1985). This ellipse can be conservatively approximated by taking as the radius of a circle the semi-major axis of said ellipse, σ_{major}. This radius is then scaled by a factor κ_{HPL} according to a central χ^2 distribution with two degrees of freedom. The resulting fault-free PL formulation is then

$$HPL_0 = \kappa_{HPL}\sigma_{major} \tag{15}$$

and describes the radius of a circle bounding the position error according to $P(PF_{PL}|H_0) < I_{risk,0}$. If a half-allocation is assumed for the fault-free and single-fault cases, a value of 5.798 for κ_{HPL} corresponds to a $1 - 0.5\text{x}10^{-7}$ probability of containing the position error. Note that the fault-free formulation in Lo, et al. (2014) is different - as they described theirs as a

preliminary PL, we have adopted the more modern formulation of (15) as our representative DME fault-free PL. This formulation is also used in SBAS GNSS, albeit with a different κ_{HPL} value corresponding to a different risk allocation, as seen in its Minimum Operational Performance Standard (SC-159, 2020).

4.2. Single-Fault Protection Level

The single-fault PL formulations are much more varied than the fault-free case, as they incorporate methods of fault detection (and occasionally exclusion) in order to protect against out-of-tolerance measurements. While the detection aspect complicates it somewhat, our task is still to relate the PL region to the allocated integrity risk.

To identify the assumptions, we again expand $P(LOI \cap H_1)$ using (9) which is further expanded to consider each measurement individually:

$$P(LOI \cap H_1) = \sum_{j=1}^{n} P\left(LOI \cap H_{1,j}\right) = \sum_{j=1}^{n} P\left(H_{1,j}\right) P\left(A' \cap PF_{PL} \middle| H_{1,j}\right) \tag{16}$$

where subscript j corresponds to measurement j. Noting that $P\left(A' \cap PF_{PL} \middle| H_{1,j}\right) = P\left(A' \middle| H_{1,j}\right) P\left(PF_{PL} \middle| A' \cap H_{1,j}\right)$, we can assume $P\left(PF_{PL} \middle| A' \cap H_{1,j}\right) = 1$ and that $P\left(H_{1,j}\right)$ is equally likely for all measurements and has the value p. We can now upper bound (16) with the expression

$$P(LOI \cap H_1) \leq p \sum_{j=1}^{n} P\left(A' \middle| H_{1,j}\right) < I_{risk,1} \tag{17}$$

where $I_{risk,1}$ is the portion of I_{risk} allocated to the single-fault condition.

At this point, we must narrow our focus somewhat. The collection of fault-detection methods developed for GNSS are referred to as Receiver Autonomous Integrity Monitoring (RAIM). The predominant single-fault formulation used in DME evaluations such as Osechas et al. (2016), Liang et al. (2022), and Osechas et al. (2022) is the max-slope residual-based RAIM (Brown & Chin, 1998). Therefore, we focus on the assumptions for that particular formulation.

Note that RAIM requires redundant measurements, or that n exceeds the number of unknown states used to determine a position solution. Max-slope RAIM uses hypothesis testing with a test statistic derived from the measurement residuals. In order to relate the statistic fault magnitudes to a position error, max-slope RAIM identifies a "worst-case" measurement where, for a given fault magnitude on this measurement, the position error is at a maximum. When plotted on a graph of statistic magnitude vs. position error, the worst-case measurement manifests as the steepest slope. Relating this to (17) is achieved as follows.

Assume the probability of no alert conditioned on the worst-case measurement is at a maximum versus all other measurements, and call this the probability of missed detection, P_{MD}:

$$P_{MD} = \max\left[P\left(A' \middle| H_{1,j}\right)\right] \tag{18}$$

From this we can further bound (17) like so:

$$P(LOI \cap H_1) \leq npP_{MD} < I_{risk,1} \tag{19}$$

The P_{MD} can then be computed by

$$P_{MD} = \frac{I_{risk,1}}{np} \tag{20}$$

This probability applies to each independent hypothesis test in the snapshot approach (Lee et al., 1996). This paper also applies P_{MD} to each snapshot, but it might be the case that this probability must be allocated to each test using an effective number of samples, as discussed in Milner et al. (2020) for the case of GNSS. In the max-slope approach, a bias on the test statistic is increased until the CDF of the faulted distribution using the threshold as input is less than P_{MD}. The corresponding bias, the so-called minimum detectable bias (MDB), is then projected into the horizontal position domain. Various simulations showed such a formulation did not meet P_{MD} as biases just less than the MDB are undetected with a greater probability while being nearly as likely to result in a position failure. Therefore, a buffer term is usually added by adding to the projected MDB the radius of a circle bounding the position error with a probability of $1 - P_{MD}$. The resulting single-fault formulation is then

$$HPL_1 = \lambda_{MDB}|_{horiz} + \kappa_{MD}\sigma_{major} \tag{21}$$

where $\lambda_{MDB}|_{horiz}$ represents the projected MDB and $\kappa_{MD}\sigma_{major}$ is the buffer term. Various max-slope formulations use different, but analogous, buffer terms. The single-fault HPL_1 defines the radius of a circle centered on the true position which the position error exceeds *unannounced* with a probability of less than $I_{risk,1}$.

Again assuming a half-allocation of 0.5x10^{-7}/hr for $I_{risk,1}$ and $p = 10^{-6}$/hr, we compute P_{MD} as 0.005 using (20) in the case of ten measurements. As the allowable P_{MD} increases (resulting in a smaller MDB) with fewer measurements, ten is a conservative value for most DME architectures. This corresponds to a value of 3.255 for κ_{MD}.

Other faulted PL formulations such as solution separation can apply to DME, and we anticipate a future paper investigating this approach for DME and other non-GNSS systems.

5. DME PROTECTION LEVEL EVALUATION

Now that the DME PLs have been explicitly connected to the overall PL framework, we can evaluate the achievable performance over Europe at FL100 (10,000ft altitude MSL). The integrity-related values selected in the previous sections are summarized in Table 2 below.

Table 2

Assumed integrity requirement values

Description	Notation	Value
Specified integrity risk	I_{risk}	10^{-7}/hr
Fault-free and single-fault allocations	$I_{risk,0}$, $I_{risk,1}$	0.5x10^{-7}/hr
Measurement fault probability	p	10^{-6}/hr
Number of measurements for P_{MD}	n	10
Probability of missed detection	P_{MD}	0.005
Probability of false alert	P_{FA}	1x10^{-8}/sample

The last row of the above table introduces a probability not yet discussed. While this paper has focused on integrity, it is difficult to completely divorce that focus from other navigation requirements like continuity. Continuity drives the specified probability of false alert, which in turn drives the test threshold in the fault detection of our single-fault PL. The selected value of 1x10^{-8}/sample for P_{FA} was taken from the DME evaluation of Liang et al. (2022), and its derivaton is described there in more detail.

For the evaluation, we assume the DME slant-range errors are zero-mean Gaussian distributed with a standard deviation of 180m, which is approximately equal to the value given in Appendix C of DO-236 (EUROCAE, 2014), and that the transmit range of a DME signal is 100 nautical miles (nmi). The DME stations are derived from a DME database provided by EUROCONTROL where we excluded TACAN, VORTAC, and ILS DME stations, with the remaining stations numbering 896. As the number of visible DME stations can be quite high, any points where more than ten stations are visible led to a random selection of ten when computing a single-fault PL.

The evaluation results are in terms of achievable RNP category. To determine this, the PLs are compared to the AL as in (7). The ALs for each RNP category are generally twice the RNP designator (e.g. 1 in RNP1) which is also the 95% accuracy requirement given in nautical miles (EUROCAE, 2014). The ALs for RNP 0.3, RNP 1, and RNP 2 are thus 0.6nmi, 2nmi, and 4nmi, respectively. The RNP ALs are also allocated to other position errors external to the navigation system, such as flight technical error (FTE). The PLs are in practice compared to a reduced AL where the allocation to FTE has been removed, but the amount of reduction depends on a particular phase of flight and mode of pilot assistance, as described in the PBN Manual (ICAO, 2013). The evaluation here makes no assumptions regarding these aspects and therefore compares the PLs to the full RNP AL. The results of the evaluation are shown in Figure 1 and Table 3 below.

Figure 1

Predicted RNP level using (left) fault-free protection level (right) single-fault protection level

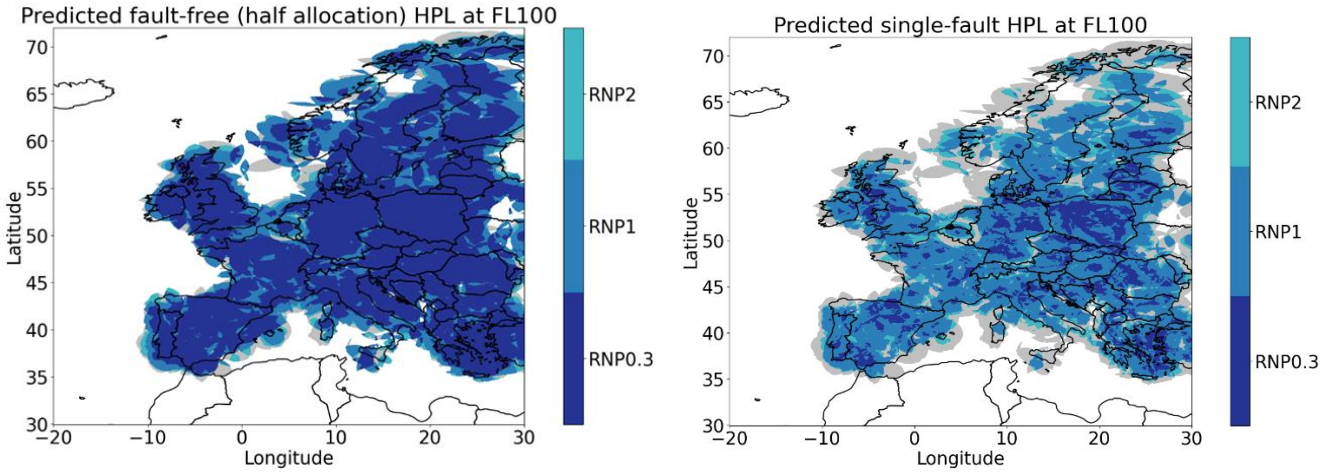

Table 3

RNP coverage as percent of area with at least three visible stations

Protection level	RNP 0.3	RNP 0.3 or RNP 1
Fault-free, HPL_0	67.1%	91.8%
Single-fault, HPL_1	13.5%	64.6%

It is important to note RNP requirements encompass more than just the integrity requirement, and that complying with integrity is a necessary but not sufficient condition for overall RNP compliance. When this paper describes a scenario as showing RNP compliance, what is meant is that the integrity requirement alone is predicted to be met based on the PL and AL comparison.

The plots in Figure 1 show that the single-fault PL should be taken as the effective PL due to its larger magnitude based on it having less coverage at RNP 0.3. The fault-free PL, given a good station geometry, reaches RNP 0.3 quite often, which agrees with the results in Lo et al. (2014) despite the slightly different formulation. This could motivate manufacturers to achieve a lower probability of concurrent DME station and monitoring function failure, as this results in a single-fault PL being unnecessary as long as propagation effects are effectively mitigated. For certain routes and operations, regular flight inspection could allay some of these propagation effect concerns.

In the single-fault case, at least RNP 1 is achieved for over 60% of the area with at least three visible stations, with most of the no-coverage areas found on the edges. As RNP 1 is a target for DME-based positioning, such a result supports more detailed analyses for particular terminal areas. When one considers that actual DME slant-range performance is likely to be much better than the 180m standard deviation used here, the results are even more promising (Vitan et al., 2015). Additionally, the max-slope RAIM method is not necessarily the optimal formulation. Solution separation, used in the ARAIM algorithm, might offer a tighter protection level (Joerger et al., 2014).

6. CONCLUSION

With DME being considered as a potential RNP system, studies have been performed evaluating its integrity performance using the protection levels developed for augmented GNSS. This paper has connected the DME protection levels to a general integrity/protection level framework, thereby making certain assumptions explicit. We showed that a protection level for a multiple fault condition is not necessary, due to the executive monitoring capability of DME. Our evaluation shows that the DME network can provide at least RNP1 at FL100 for the majority of Europe with the max-slope RAIM method computing a single-fault protection level. Formulating DME protection levels in the general framework revealed the improvement offered by the sole fault-free protection level, should the concurrent failure and propagation fault probabilities be low enough. More detailed analyses are required to evaluate the integrity performance of DME for particular terminal areas. Such analyses should

consider if a max-slope RAIM approach is optimal, as well as if the missed detection probability should be adjusted to consider an effective number of samples. Lastly, as DME is likely to be combined with other sensors such as barometric altimeters, the impact of multiple sensors on the protection level framework must be shown before inclusion in any PL formulation.

7. ACKNOWLEDGEMENTS

The authors would like to thank Vali Vitan and Gary Berz of EUROCONTROL for providing the DME station database as well as their insightful comments regarding the DME monitoring architectures.

8. REFERENCES

Berz, G., & Saini, L. (2022). Reengineering DME/N Integrity to Support PBN. *International Flight Inspection Symposium.* Durban, South Africa.

Berz, G., Vitan, V., Skyrda, I., & Ober, P. (2013). Can Current DME Support PBN Operations with Integrity? *Proceedings of the 26th International Technical Meeting of the ION Satellite Division, ION GNSS+ 2013*, (pp. 233-250). Nashville, Tennessee.

Blanch, J., Walter, T., Enge, P., Lee, Y., Pervan, B., Rippl, M., & Spletter, A. (2012). Advanced RAIM user Algorithm Description: Integrity Support Message Processing, Fault Detection, Exclusion, and Protection Level Calculation. *Proceedings of the 25th International Technical Meeting of the Satellite Division of The Institute of Navigation (ION GNSS 2012).* Nashville, TN.

Brown, R. G., & Chin, G. Y. (1998). GPS RAIM: Calculation of Thresholds and Protection Radius Using Chi-Square Methods - A Geometric Approach. In *Global Positioning System (ION Red Book): Vol. V* (pp. 155-178). Fairfax, VA: Institute of Navigation.

DeCleene, B. (2000). Defining Pseudorange Integrity - Overbounding. *Proceedings of the 13th International Technical Meeting of the Satellite Division of The Institute of Navigation.* Salt Lake City, UT.

Department of Defense, Department of Transportation, and Department of Homeland Security. (2021). *Federal Radionavigation Plan (DOT-VNTSC-OST-R-15-01).* Springfield, VA.

European and North Atlantic Office of ICAO. (2019). *European Guidance Material on Integrity Demonstration In Support of Certification of ILS and MLS Systems (ICAO EUR DOC 016).* Neuilly-sur-Seine, France: International Civil Aviation Organization.

European Organisation for Civil Aviation Equipment. (2014). *Minimum Aviation System Performance Standards: Required Navigation Performance for Area Navigation (ED-75D).* Malakoff, France.

International Civil Aviation Organization. (2013). *Performance-based Navigation (PBN) Manual (Doc 9613).* Montréal, Canada.

International Civil Aviation Organization. (2018). *Annex 10 to the Convention on Civil Aviation - Aeronautical Telecommunications: Vol. I Radio Navigation Aids* (7th ed.). Montreal, Canada.

Joerger, M., Chan, F.-C., & Pervan, B. (2014). Solution Separation Versus Residual-Based RAIM. *NAVIGATION: Journal of the Institute of Navigation, 61*(4), 273-291.

Lee, Y., Van Dyke, K., Decleene, B., Studenny, J., & Beckmann, M. (1996). Summary of RTCA SC-159 GPS Integrity Working Group Activities. *NAVIGATION: Journal of The Institute of Navigation, 43*(3), 307-338.

Liang, X., Milner, C., Macabiau, C., & Estival, P. (2022). Multi-DMEs for alternative postition, navigation and timing (A-PNT). *The Journal of Navigation, 75*(3), 625-645.

Lo, S., Chen, Y.-H., Zhang, S., & Enge, P. (2014). Hybrid APNT: Terrestrial Radionavigation to Support Future Aviation Needs. *Proceedings of the 27th International Technical Meeting of the Satellite Division of the Institute of Navigation (ION GNSS+ 2014).* Tampa, Florida.

Mertikas, S. P. (1985). *Error Distributions and Accuracy Measures in Navigation: An Overview (Technical Report No. 113).* Department of Surveying Engineering, University of New Brunswick.

Milner, C., Pervan, B., Blanch, J., & Joerger, M. (2020). Evaluating Integrity and Continuity Over Time in Advanced RAIM. *2020 IEEE/ION Position, Location, and Navigation Symposium (PLANS)*, (pp. 502-514). Portland, OR.

Osechas, O., Nossek, E., Belabbas, B., & Meurer, M. (2016). A Modular Approach to Integrity for APNT. *Proceedings of the 29th International Technical Meeting of the Satellite Division of The Institute of Navigation (ION GNSS+ 2016)*, (pp. 2293 - 2299). Portland, OR.

Osechas, O., Zampieri, G., Weaver, B., Felux, M., Dehaynain, C., Berz, G., . . . Maurizio, S. (2022). A Standardizeable Framework Enabling DME/DME to Support RNP. *Proceedings of the 35th Internation Technical Meeting of the Satellite Division of The Institute of Navigation (ION GNSS+ 2022).* Denver, CO.

Pullen, S., & Joerger, M. (2021). GNSS Integrity and Receiver Autonomous Integrity Monitoring (RAIM). In *Position, Navigation, and Timing Technologies in the 21st Century* (pp. 591-617). Hoboken, New Jersey: John Wiley & Sons, Inc.

SC-159. (2020). *MOPS for GPS/Wide Area Augmentation System (WAAS) Airborne Equipment (RTCA DO-229F, Paper No. 083-20/SC159-1083).* Washington D.C.: RTCA, Inc.

Vitan, V., Berz, G., & Solomina, N. (2015). Assessment of current DME performance and the potential to support a future A-PNT solution. *2015 IEEE/AIAA 34th Digital Avionics Systems Conference (DASC)*, (pp. 2A2-1-2A2-18). Prague, Czech Republic.

Walter, T., Enge, P., & Hansen, A. (1999). Integrity Equations for WAAS MOPS. In *Global Positioning System: Papers Published in NAVIGATION* (Vol. VI). The Institute of Navigation.